*Ann. Rev. Astron. Astrophys. 1983. 21: 109–30*






# EVIDENCE FOR LOCAL ANISOTROPY OF THE HUBBLE FLOW

*Marc Davis*

Astronomy and Physics Departments, University of California, Berkeley, California 94720

*P. J. E. Peebles*

Joseph Henry Laboratories, Princeton University, Princeton, New Jersey 08544 and Dominion Astrophysical Observatory, Victoria, British Columbia V8X 3X3, Canada

## 1. INTRODUCTION

The Universe is accurately isotropic when measured by radio source counts and deep galaxy counts, or by the integrated microwave and X-ray backgrounds. On the other hand, galaxies are distributed in a decidedly clumpy way on scales of a few tens of megaparsecs, and it is natural therefore to ask whether galaxy redshifts show systematic departures from Hubble's law when averaged over similar scales. Discussions of this question have tended to develop along lines fixed by ideas for what might be reasonable patterns of deviations from Hubble's law. If the coherence length of the effect is large enough, it makes sense to expand the redshift field in a power series in distance, just as Oort (55) did for the velocity field in the Galaxy. This has been a convenient approach in theoretical discussions, but so far has proved to be only moderately useful as a framework for analysis of the data, perhaps because one coherence length contains too few independent groups of galaxies. A second framework is based on the thought that the mass concentration in a cluster of galaxies might induce a more or less radial flow toward the cluster in the surrounding field (24). In



0066–4146/83/0915–0109$02.00

particular, the bright galaxies are concentrated toward the Virgo cluster, forming a system that, after Shapley (82) and de Vaucouleurs (23, 24), has come to be called the Local Supercluster (hereinafter called the LS). One can ask whether the gravitational acceleration of the mass concentrated in this system has given us an appreciable peculiar Virgocentric velocity $v_v$. As the LS appears flat, one can also ask whether the velocity field has appreciable circulation. These questions were posed, and answers proposed, by de Vaucouleurs (24). Following the trend of recent discussions, we focus this review on the first question. It appears that $v_v$ is detected in the redshift data, and is comparable to the value originally proposed by de Vaucouleurs.

The value of $v_v$ is of interest as one measure of the accuracy of Hubble's law, and also as a measure of the mass of the LS (24, 74). This is particularly important as a clue to the mass of the universe. It is fairly well established that the dark mass clustered around bright galaxies on scales $\sim 30$–$300\ h^{-1}$ kpc is about ten times the mass seen within the galaxies (assuming Newton's laws are accurate approximations!) (21, 34). The dynamics of the LS represents the best near-term hope for a measure of the component of mass that might be clustered only on scales $\sim 10\ h^{-1}$ Mpc. We conclude below that the behavior of this system does indicate mass in excess of what is seen concentrated around galaxies on scales $\lesssim 1$ Mpc.

We write Hubble's law as the vector equation

$$\mathbf{v} = H\mathbf{r}, \qquad H = 100\,h\ \mathrm{km\ s^{-1}\ Mpc^{-1}}, \tag{1.}$$

where $z = v/c$ is the redshift. This has come to be called pure or ideal Hubble flow (74). The dimensionless parameter $h$ is thought to be in the range 0.5 to 1. As typical values of $v$ are much less than $c$, we ignore space curvature and other relativistic effects.

## 2. MODELS FOR DEPARTURE FROM HUBBLE FLOW

We describe here some of the history of ideas on departures from pure Hubble flow. In the next section, we discuss the use of models as frameworks for analysis of the observations. One approach is to analyze the degree of isotropy of redshifts of the galaxies at a given range of distances, perhaps by expansion in spherical harmonics. If the $Y_1^m$ (dipole) terms dominate, the natural interpretation is that we are seeing the effect of our peculiar velocity relative to the shell. If this velocity varies with shell radius, it can be interpreted to mean that we are seeing a smoothly varying velocity field. The dipole anisotropy term played a central role in the first discussions of the pattern of galaxy redshifts (48, 94), but after it was seen that Hubble's law gives a good first approximation to the redshifts, people tended to conclude that large-scale currents must be fairly small, and so they concentrated on the solar motion relative to galaxies in the Local Group or close to it (17). More recently, de Vaucouleurs & Peters (29) studied the dipole anisotropy of the galaxies at depths comparable to that of the LS, and Rubin et al. (67) introduced the study of the dipole anisotropy of galaxy redshifts at depths well beyond the LS. By this time it was recognized that the diffuse microwave background radiation ought to show the same dipole anisotropy effect (56, 60), and that it would be very interesting to compare the solar motion it implies to the motion derived from galaxy redshifts (29, 80, 89). As described below, it appears that the solar motion relative to the very large-scale frame of reference defined by the microwave background is at least roughly comparable to the motion relative to the LS.

## 2.1 *First-Order Expansion*

If the galaxies defined a smoothly varying peculiar velocity field $\mathbf{V}(\mathbf{r})$, then at small enough distances $r$ the relative velocity field is

$$V^{\alpha}(\mathbf{r}) - V^{\alpha}(0) = \sum r^{\beta} \partial V^{\alpha}/\partial r^{\beta},$$

where the indices represent Cartesian components. We can write the second term as the sum of a uniform expansion $H_e r^{\alpha}$, where $H_e$ need not agree with Hubble's constant; a shear term $\sigma_{\alpha\beta} r^{\beta}$, where $\sigma_{\alpha\beta}$ is symmetric and traceless; and a rotation $\omega_{\alpha\beta} r^{\beta}$, with $\omega_{\alpha\beta} = -\omega_{\beta\alpha}$. The last term is not observable in the line-of-sight velocity but if present acts as a kinematic source for the shear (58; Equation 20.22). Since $\sigma_{\alpha\beta}$ is symmetric, we can orient the coordinate axes so $\sigma$ is diagonal, and the relative line-of-sight velocity becomes

$$V_r = r[H_e + a \sin^2 \theta \cos 2\phi + b(1 - 3 \cos^2 \theta)], \qquad 2.$$

to first order in distance $r$. The solar motion relative to the mean streaming field adds a constant dipole term to this quadrupole anisotropy.

Lemaître (46), Gamow (39), Gödel (40), and Schücking (79) were among the first to discuss cosmological models in which shear might produce the quadrupole anisotropy in Equation 2, and Rubin (63, 64) and Ogorodnikov (53) were the first to test for such an effect in the galaxy redshift data. Rubin and Ogorodnikov were guided in part by Oort's linear expansion of the star streaming field in the Galaxy, as was proposed earlier by Gamow (39). They considered the possibility that we are in a very large structure expanding and shearing around an unspecified distant center, though Rubin did take note of the concentration of galaxies along the plane of the LS. It was de Vaucouleurs (24), and independently Carpenter (as communicated to

Rubin), who proposed that we may be able to detect the shear due to the peculiar velocity field around a specific object, namely the LS.

As the data available to Rubin and Ogorodnikov were sparse, it is not surprising that their results do not agree with each other or with more recent opinions on $\sigma_{\alpha\beta}$, but their work is of considerable interest as early steps in an active tradition. Steward & Sciama (80, 89) used Equation 2 in a test for shear associated with the LS. Kristian & Sachs (45) discussed the quadrupole anisotropy associated with possible very large-scale inhomogeneities, and they used the redshift catalog of Humason, Mayall & Sandage to find an informal limit on the dimensionless shear $\sigma/H$. The considerable recent progress in the theory of anisotropic relativistic world models is reviewed by MacCallum (49).

## 2.2 *DeVaucouleurs' Model for Flow in the Local Supercluster*

De Vaucouleurs (24) noted that the gravitational attraction of the mass concentration in the LS might be expected to slow the general expansion in the field nearby. Since the LS appears flattened, he noted that one might also look for circulation. He proposed as reasonable working models for the two components of flow in the plane the functions

$$v_r = H_0 R(1 - e^{-R/R_1}), \qquad \omega(R) = \omega_0 \exp -(R/R_1)^2. \qquad 3.$$

Here $R$ is the distance from the center of the system and $R_1$ is the distance to the Local Group. In this model the radial velocity $v_r \ll H_0 R$ at small $R$, as is appropriate for the relaxed central parts of the system. The local radial peculiar velocity is $v_v = H_0 R_1/e \sim 550$ km s$^{-1}$, which is somewhat higher than the more recent estimates described in the next section. His estimate of the transverse velocity was $R_1\omega_1 \sim 500$ km s$^{-1}$. A subsequent analysis (29) with a larger redshift sample yielded $R_1\omega_1 = 400 \pm 100$ km s$^{-1}$, and tentatively identified a component $v_z \sim 300$ km s$^{-1}$ normal to the plane of the system.

## 2.3 *Gravitational Perturbation Models*

Many of the recent studies of the galaxy redshift field in the LS use models derived from the gravitational theory of the velocity field around a mass concentration in a Friedman-Lemaître world model. This effect was discussed by Silk (83), who obtained a relation between the local expansion $\nabla \cdot \mathbf{V}$, the local density contrast $\delta\rho/\rho$, and the cosmological density parameter $\Omega$. Silk's results, which are based on Raychaudhuri's (61) equation, are general and powerful tools for analyzing the evolution of density irregularities, but because they refer to local quantities they are not directly useful for analysis of the redshift field around a cluster. The following treatment was first developed (in the linear approximation) and applied to an analysis of the redshift field around the LS by Peebles (57).

Since our Virgocentric velocity $v_v$ is small compared to the Hubble velocity $H_0R_1$, linear perturbation theory should give a useful approximation to the behavior of the velocity field near us. On the other hand, the mean density of galaxies within $R_1$ is about three times the large-scale mean (20), so nonlinear corrections may be expected to be significant. We shall use the linear approximation to discuss the basic properties of the velocity field, and then review some aspects of nonlinear calculations.

The peculiar gravitational field is

$$\mathbf{g} = G\int d^3x'(\rho(\mathbf{x}')-\rho_b)(\mathbf{x}'-\mathbf{x})/|\mathbf{x}'-\mathbf{x}|^3. \qquad 4.$$

In linear perturbation theory, the resulting peculiar velocity is (58; Section 14)

$$\mathbf{v} = 2f\mathbf{g}/(3H_0\Omega), \qquad 5.$$

and the net proper displacement of a mass element is

$$\delta\mathbf{r} = \mathbf{g}/(4\pi G\rho_b). \qquad 6.$$

Here $\Omega$ is the cosmological density parameter (the mean mass density $\rho_b$ divided by the Einstein-de Sitter density) and the function $f(\Omega)$ is discussed in (58; Section 14). If the cosmological constant $\Lambda$ is negligible, $f \sim \Omega^{0.6}$. These equations assume nongravitational forces are negligible now and have been for some time in the past so the growing mode dominates.

Estimation of the expected peculiar velocity is greatly simplified if $\mathbf{g}$ is close to radial. Though the galaxy distribution in the LS is quite irregular, this may still be a useful approximation. For example, if the mass were in a flat homogeneous spheroid the acceleration at the rim would be $g_{edge} = (3\pi/4)g_s = 2.4\ g_s$, where $g_s$ is the acceleration of the same mass in a sphere at the same radius, and the acceleration along the normal to the disk at the same distance from the center would be $g_n = 0.644\ g_s$. This illustrates the point that the gravitational potential is much closer to spherical than is the mass distribution, and that the error in using the spherical model to estimate $g$ for given mass and radius tends to be modest, amounting to a factor $\sim 2$ in this fairly extreme case.

In the spherical model, Equation 5 is

$$v_v = \frac{2G\delta M}{3H_0R^2\Omega^{0.4}}, \qquad 7.$$

where $\delta M$ is the mass excess within the radius $R$. Thus, from $v_v$ we can estimate the very interesting quantity $\delta M$ (within conventional gravity physics!) up to the uncertainties due to $\Omega$ and the spherical model. These are relatively mild compared with the uncertainty in the mass we expect to find within the LS, based on our understanding of galaxy masses.

If mass is clustered like galaxies on scales $\sim 10\ h^{-1}$ Mpc we can rewrite Equation 7 as

$$v_{\mathrm{v}} = \tfrac{1}{3}H_0 R\Omega^{0.6}\delta N/N, \qquad 8.$$

where $\delta N/N$ is the fractional excess of the galaxy count within $R$ relative to what is expected for a homogeneous Universe. This equation fixes the density parameter in terms of the two quantities, $v_{\mathrm{v}}$ and $\delta N/N$, which are in principle measurable.

Estimates of the $v_{\mathrm{v}}$ expected in the nonspherical linear model (Equation 5) have been made from the observed galaxy distribution, assuming that mass and light are correlated on large scales (20, 106). If $\delta N/N \sim 2$, as is suggested by the latest observations (20), then in linear theory $v_{\mathrm{v}} \sim 670\ \Omega^{0.6}$ km s$^{-1}$ and is directed $\sim 20°$ northwest of Virgo.

The variation of the peculiar velocity with distance $R$ from the cluster center has been estimated from a power-law model for the mass density run, $\rho(R) \propto R^{-\gamma}$, with $\gamma \sim 2$. This agrees with the average for Abell clusters (81), and is not inconsistent with the galaxy counts around the Local Supercluster (95, 106). In this model, $v_{\mathrm{v}} \propto R^{-(\gamma-1)}$ (57).

In the zero-pressure spherical model it is straightforward to correct these results for nonlinear behavior (58, Section 19; 22, 44, 54, 78, 84, 93, 105). Figure 1 shows the ratio of the peculiar velocity $v_{\mathrm{v}}$ to the Hubble velocity $HR$. The parameter labeling each pair of curves is the fractional mass excess $\delta M/M = M/M_{\mathrm{b}} - 1$, where $M$ is the mass within $R$ and $M_{\mathrm{b}}$ the mass

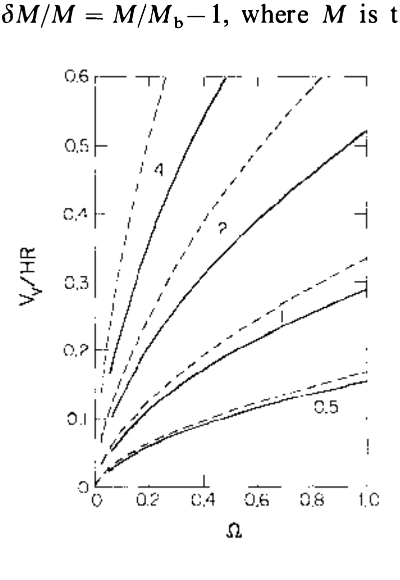


*Figure 1* Peculiar velocity in the zero-pressure spheroidal model. The parameter is the fractional mass excess $M/M_{\mathrm{b}} - 1$. The dashed curves are the linear approximations (Equation 8), and the solid curves are the full nonlinear model.

expected for a homogeneous distribution. The solid curves are based on the spherical zero-pressure model, and assume that mass shells do not cross and that $\delta M/M \rightarrow 0$ at high redshift. The dashed curves are the linear approximation in Equation 8. The exact and linear relations are not greatly different. For example, at $\delta M/M = 4$ the values of $v_v$ at fixed $\Omega$ differ by a nearly constant factor 1.4 and the values of $\Omega$ at fixed $v_v$ differ by the nearly constant factor 1.8. A more serious problem is that at fixed $\Omega$ the error in $v_v$ increases with increasing $\delta M/M$, which affects the predicted run of $v_v$ with $R$ for a given mass distribution.

Figure 2 shows the redshift pattern around the LS in a nonlinear spherical model (93). Initial conditions have been adjusted so that the present density run is $\rho - \rho_b \propto R^{-2}$; the virgocentric velocity at our position is $v_v = 400$ km s$^{-1}$, and $\delta M/M = 2$. The effect on the redshift field appears at $r \ll R_1$
$3H_0$ and in the quadrupole anisotropy of Equation 2. Near the center of the system the flow is complicated, with some redshifts appearing at three distances. At $r \gg R_1$

The behavior of the flow at $R < R_1$

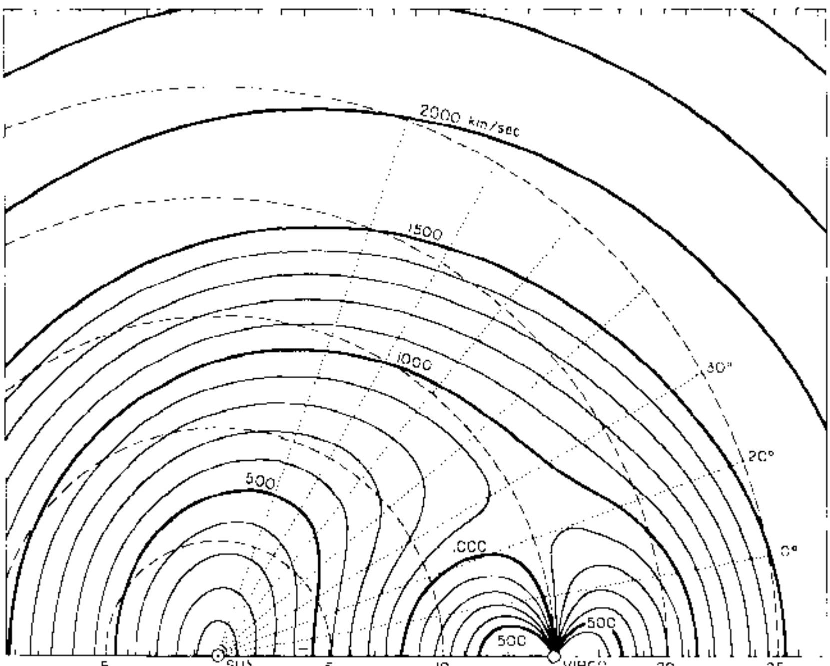


*Figure 2* The redshift field around the LS in a spherical nonlinear gravitational model (93).

complicated than in this spherical model, however, because of a second important nonlinear effect. Although the gravitational field tends to be roughly radial even for a strongly anisotropic mass distribution, the resulting velocity field is kinematically unstable against diverging shear in a caustic surface or pancake. This is seen in the behavior of homogeneous ellipsoids (58, Section 20; 103) and in Zel'dovich's kinematic analysis (58, Section 21; 108). The velocity field tends to become substantially out of line with the local direction of gravity when the fractional displacement $\delta R_1/R_1$ is on the order of unity. In the spherical approximation, this displacement is $\delta R/R \sim (M/M_b)^{1/3}-1$. At our position, $M/M_b \sim 3$, so $\delta R_1/R_1 \sim 0.4$, which indicates that the spherical model may be expected to be a useful but somewhat rough approximation. At $R = R_1/2$, $M/M_b \sim 9$, so $\delta R \sim R$, and orbits therefore may be expected to be decidedly nonradial. Thus, the presence of the triple-valued region in Figure 2 at $R < R_1/2$ should be taken to mean only that the flow here is likely to be exceedingly complicated. An example is a model in which the LS has completed collapse along one axis while still expanding along the other two (85).

If the Universe is dominated by massive neutrinos or other massive weakly interacting particles, the mass distribution in the LS could be very different from that of the galaxies. Hoffman et al. (44, 44a) have discussed spherical collapse models that are designed to be fit to the mass distribution as indicated by the velocity dispersion of the galaxies rather than by the velocity distribution itself. In a neutrino-dominated Universe, the dissipationless neutrinos could be considerably less clumped than the baryonic galaxies, even on the scale of the LS (12, 85).

## 3. EVIDENCE FOR ANISOTROPY

We have ordered this section roughly by distance. For the more distant objects, people have concentrated on the dipole anisotropy due to our peculiar motion. For relatively nearby objects, more details of the velocity field are in principle observable but one must then deal with more parameters in the model for the velocity field.

### 3.1 *Extremely Distant*

The microwave and X-ray backgrounds provide frames of reference against which we can measure our peculiar velocity. Even if the Universe is accurately isotropic the backgrounds can appear isotropic only to a comoving observer: the Lorentz transformation to an observer moving at speed $v \ll c$ yields

$$\frac{\delta i}{i} = \left(3 - \frac{v}{i}\frac{di}{dv}\right)\frac{v}{c}\cos\theta,$$

where $i$ is the brightness (ergs cm$^{-2}$ s$^{-1}$ ster$^{-1}$ Hz$^{-1}$) and $\theta$ is the angle from the direction of motion. For the 1–10 keV X-ray background, $\delta i/i \cong 3.5(v/c) \cos \theta$. The microwave background has a nearly thermal spectrum, so $\delta i/i = (v/c) \cos \theta$ at long wavelengths and at all wavelengths $\delta T/T = (v/c) \cos \theta$, where $T$ is the thermodynamic temperature (60).

The anisotropy of the microwave background has been convincingly detected and is close to a pure dipole field, the quadrupole part being $\lesssim 8\%$ of the dipole amplitude (18, 37, 41, 47, 87). [An earlier report of a larger quadrupole anisotropy (13) that could have been due to the Sachs-Wolfe effect (59, 86) seems to have been due to imperfect correction for emission from the Galaxy.] The amplitude $\delta T/T$ is independent of wavelength within the accuracy of the measurements. These observations are strong evidence that the effect is the result of our peculiar motion in a Universe that is very nearly spherically symmetric on the horizons. With the estimate of Yahil et al. (107) for the solar motion relative to the Local Group, we find that the components of the velocity of the Local Group are (in km s$^{-1}$)

$$(v_v, v_s, v_z) = (410 \pm 25, 297 \pm 25 - 308 \pm 25), \qquad 9.$$

where $v_v$ is the component directed toward Virgo, $v_s$ is directed transverse to Virgo but in the plane of the LS, and $v_z$ is transverse to Virgo and the LS plane. We list values of $v_v$ in Table 1.

The HEAO I X-ray anisotropy measurements are consistent with the microwave results, but as the correction for the Galactic contribution is large this is not yet an independent confirmation of the effect (11a).

## 3.2 *Very Distant*

The redshift-magnitude relation for rich clusters at $0.02 \lesssim z \lesssim 0.3$ has been extensively studied by Sandage and his colleagues (68, 69, 71). They find that on the assumption of pure Hubble law the absolute magnitudes of the brightest cluster members have an rms spread of 0.3 mag. This means that Hubble's law fits the data to $\sim 15\%$ (standard deviation) in redshift.

The brightest elliptical in the Virgo cluster, N4472, falls very close to the mean relation, which is evidence that peculiar velocities have had negligible effect on the redshift of the Virgo cluster (68, 69, 71). Since the Virgo cluster is not very rich, one might expect that N4472 is, if anything, less luminous than the mean, which would be evidence that $v_v$ is negative. However, the richness correction is contentious (42), so this perhaps is not a strong point. The estimate and standard deviation of $v_v$ in Table 1 are interpolated from the analysis of Aaronson & Mould (3), who used the Hubble relation of Sandage et al. (69a) and the observed magnitudes of N4472 corrected for each $v_v$ to a fixed linear aperture. It is assumed that the luminosity of N4472 is drawn from an unbiased sample for rich clusters with standard deviation

**Table 1** The velocity of the Local Group toward Virgo

| Method | $v_v$ | References |
|---|---|---|
| 1. Microwave background | $410 \pm 25^{a}$ | (37, 47) |
| 2. Hubble line for clusters | $150 \pm 200^{b,c}$ | (3, 69a) |
| 3. Sc I gal. at $cz \sim 4000$ | $-90 \pm 150^{a}$ | (75, 76) |
| 4. $M_H$–$\Delta v$ at $cz \sim 2500$ | $450 \pm 55^{a}$ | (43) |
| 5. $\Delta m_{cv}$: photographic luminosity function | $40 \pm 160^{c}$ | (33) |
| 6. $\Delta m_{cv}$: nuclear magnitudes of bright galaxies | $30 \pm 160^{c}$ | (102) |
| 7. $\Delta m_{cv}$: $B_T$ of bright galaxies | $400 \pm 300^{c}$ | (5) |
| 8. $\Delta m_{cv}$: colors of bright galaxies | $230 \pm 140^{c}$ | (101) |
| 9. $\Delta m_{cv}$: colors of bright galaxies | $340 \pm 110^{c}$ | (6) |
| 10. $\Delta m_{cv}$: supernovae | $40 \pm 160^{c}$ | (15, 72) |
| 11. $L$–$\Delta v$ at $cz \sim 5000$ | $520 \pm 75^{c}$ | (5, 51) |
| 12. $L$–$\sigma$ at $cz \sim 5000$; E | $470 \pm 75^{c}$ | (92, 93) |
| 13. $L$–$\sigma$ at $cz \sim 5000$; S0 | $416 \pm 90^{c}$ | (92, 93) |
| 14. $B_T$ at $cz \sim 1000$ | $175 \pm 60^{e}$ | (30) |
| 15. $B_T$–$\Delta v$ at $cz \sim 1000$ | $197 \pm 40^{e}$ | (31) |
| 16. Local: Sc I galaxies | $500 \pm 150^{d}$ | (57) |
| 17. Local: RSA | $220 \pm 75^{d}$ | (105) |
| 18. IR–$\Delta v$: $\Delta m$ for Fornax & Virgo | $316 \pm 80^{d}$ | (2, 7) |
| 19. IR–$\Delta v$: flow model | $331 \pm 41^{d}$ | (2) |
| 20. IR–$\Delta v$: flow model plus noise | $250 \pm 64^{d,f}$ | (2) |

[a] Assumes the Virgo cluster has negligible peculiar velocity.
[b] Richness correction may reduce $v_v$.
[c] If the observed Virgo redshift corrected to the Local Group is $980 + \Delta$, subtract $\Delta$ from $v_v$.
[d] Assumes Virgocentric flow $v \sim R^{-1}$.
[e] Dipole fit.
[f] Pattern velocity.

0.3 mag, and that the cosmological redshift of the Virgo cluster corrected to the Local Group is (51, 105, 107)

$$cz_v = 980 \pm 51 \text{ km s}^{-1} + v_v. \tag{10}$$

For further discussion, see references (1) and (3).

## 3.3 *Intermediate Scales*

Objects at redshifts $3000 \lesssim cz \lesssim 10{,}000$ km s$^{-1}$ have been studied using a broad variety of distance indicators. Here the goal has been to estimate our motion relative to the frame defined by the sample, or, by comparing the object with similar-looking ones in the Virgo cluster, to scale the cosmological redshift of the LS and hence find $v_v$ on the assumption that the deeper objects have negligible peculiar velocities. Excellent recent reviews from opposing points of view are given in (5) and (72). Older data are reviewed in (64a).

We consider first the dipole anisotropy of the redshifts. In a sample of Sc I galaxies at redshifts $\sim$4000–6000 km s$^{-1}$ and magnitudes $14 \lesssim m \lesssim 15$, Rubin et al. (64a, 66, 67) and Jackson (44c) found that the galaxies in the northern sky had systematically higher velocities, as if the Local Group had a velocity relative to this sample $\sim$600 km s$^{-1}$ directed almost orthogonal to that derived from the microwave background. Schechter (77) reanalyzed the data, finding a similar mean velocity and a somewhat larger uncertainty. A similar analysis applied to a closer, brighter sample led to results that disagreed in direction and amplitude. This could mean that there is considerable noise in the redshift field even on scales $cz \sim$ 6000 km s$^{-1}$ (19), or else that the results are questionable. Fall & Jones (36) argued for the latter, noting that a combination of an underestimation of the dispersion of the intrinsic luminosities with the known clustering of the galaxy distribution could mimic the Rubin et al. result with no peculiar velocity field required. Tammann et al. (90) showed that indeed Sc I galaxies have a considerably larger intrinsic luminosity dispersion than previous estimates.

In a similar study, Hart & Davies (43) used as a distance indicator the correlation of 21-cm line strength with line width. They sampled 84 Sbc galaxies in the redshift range 1000–5500 km s$^{-1}$. Objects in the Virgo cluster were deleted to avoid complications of the local flow pattern. They found a Local Group velocity relative to this background very close in amplitude and direction to that implied by the microwave anisotropy. This is a very powerful test because the use of an extra parameter, such as the distance-independent line width, largely removes the sensitivity of the test to spatial inhomogeneity of the objects and subsequent Malmquist biases of the sort that could have contaminated the Rubin et al. result. However, there are some possible problems. The scatter in the $M_{\rm H}$–$\Delta v$ relation amounts to $\sim$0.8 mag, which is large, and the resulting velocity errors appear to be too small for a sample of the size used. Also, they find $M_{\rm H} \propto \Delta v^a$, $a = 1.85 \pm 0.25$, whereas the usual relation from optical magnitudes is $a \sim 4$. However, when they substituted $B$ magnitudes for $M_{\rm H}$ they found essentially the same result. As a further demonstration, Hart & Davies repeated their analysis using a subset of the Rubin et al. sample of Sc I galaxies that have H I data, supplementing the sample slightly with more southern objects to improve the sky coverage. The result of the dipole fit gives a velocity of the Local Group of 580 km s$^{-1}$, consistent with their other fits but contrary to the original dipole fit of Rubin et al.

We consider next estimates of $v_{\rm v}$ based on the observed redshift of the Virgo cluster and the redshift scaled from deeper objects. A good point of reference is the relative distance modulus of the Coma and Virgo clusters. The redshift of the former is $6950 \pm 61$ km s$^{-1}$ (91), so for pure Hubble flow $\Delta m_{\rm cv} = 4.25 \pm 0.11$. If $v_{\rm v} \sim 400$, which is suggested by the Hart & Davies result, $\Delta m$ is reduced by 0.7 mag. Abell and colleagues (7–9, 11, 33) estimated $\Delta m$ using the luminosity distribution functions of Abell clusters, with magnitudes derived primarily from a technique of extrafocal photographic photometry (10). The assumption is that the luminosity function is universal and independent of cluster environment, so that one can use the apparent magnitude of the characteristic bend in the distribution function as a relative distance estimator. Eastmond (33) found $\Delta m_{cv} = 4.2$ for the early-type galaxies in the Coma and Virgo clusters. The uncertainty in this result is hard to assess. Since there may be problems in photographically comparing objects differing by four magnitudes, we adopt as a guess 0.3 mag in computing the standard deviation shown in Table 1.

Similar studies using photoelectric photometry have only been pursued to a limited extent. Weedman (102) studied nuclear magnitudes (luminosity in an aperture subtending $\sim 5$ kpc). He found that the Hubble diagram for the ten brightest members of each of nine clusters shows no evidence for significant non-Hubble velocities for clusters with redshifts $1000 < cz < 11{,}000$ km s$^{-1}$. The entry in Table 1 is based on $\Delta m_{cv} = 4.22 \pm 0.3$. The aperture correction to convert to an equal subtended size at a different distance is substantial for nuclear magnitudes, making nuclear magnitudes $\sim 1.7$ times less sensitive to $v_v$ than total magnitudes. According to Aaronson et al. (5), $B_T$ magnitudes (28), which are available for seven of the ten brightest Coma galaxies, yield $\Delta m_{cv} = 3.7 \pm 0.42$, or $v_v = 400 \pm 300$. Rubin (64a) has argued that the Weedman sample may be contaminated by Malmquist bias, because there is a trend of Hubble modulus with distance in the sample after elimination of the Virgo and Perseus clusters.

Another method uses the color-magnitude correlation of early-type galaxies (75, 76, 99–101). The conventional interpretation of this effect is that the largest galaxies are the most metal enriched and hence the reddest because of line blanketing. The presumption again is that the correlation is unaffected by environment. The effect is a tenuous one, with a slope $d(u\text{–}V)/d(M(V)) = 0.1 \pm 0.01$, so if $v_v = 400$ km s$^{-1}$ it changes the color index between Coma and Virgo by only 0.07 mag. Visvanathan & Sandage (101) studied the Hubble diagram of groups and clusters out to the distance of Coma using this method. They found $\Delta m_{cv} = 3.89 \pm 0.2$, or $v_v = 230 \pm 140$. They argue that their results are consistent with essentially no velocity field in the LS, since Virgo as well as the nearby Leo, Fornax, and Doradus groups fall on a linear Hubble relation extending through the more distant clusters of Pegasus, Centaurus, Coma, and others. A reanalysis of the Sandage & Visvanathan color-magnitude data by Aaronson et al. (5) yielded $\Delta m_{cv} = 3.72 \pm 0.15$ and $v_v = 340 \pm 110$.

Recently, however, Aaronson et al. (6), using the IR color-magnitude relation in the $u$–$K$ bands found results quite contrary to the previous studies. The $u$–$K$ correlation has a slope $d(u-K)/d(M(K)) = 0.22$, so it is twice as sensitive as the $u$–$V$ colors. They found that $\Delta m_{cv}$ depends on color band, deriving $\Delta m_{cv} = 3.5 \pm 2$, $3.0 \pm 0.2$, and $2.6 \pm 0.3$ for $u$–$V$, $u$–$K$, and $V$–$K$ colors respectively for a sample of 31 galaxies in Virgo and 22 galaxies in Coma. These values are consistent with a large $v_v$, but the dramatic differences in the IR moduli suggest that the CM correlation does not have a universal form among clusters. This is not inconceivable, since the Coma cluster is so much richer and more centrally concentrated than the Virgo cluster. This, of course, clouds the use of the CM correlation as a distance indicator unless the cluster environments are similar.

The Pegasus I group was also studied by Visvanathan & Sandage in $u$–$V$ and, based on four galaxies, they found a relative distance modulus to Virgo of $2.75 \pm 0.5$, consistent with the value of $2.96 \pm 0.08$ expected from the redshift ratio. Mould (50) applied the $u$–$K$ color-magnitude test to twelve early-type galaxies in this same cluster and found $\Delta m = 2.32 \pm 0.37$, which supports the notion of a substantial velocity field in the LS. This cluster is of low central concentration and is spiral rich, like Virgo, so perhaps the color-magnitude correlation provides a useful relative distance estimator. Further photometry will be required to clarify this situation.

Type I supernovae can easily be seen beyond the distance of Coma. Data on well-observed supernovae have been compiled by Branch & Bettis (14, 15). Type I supernovae are seen in all types of galaxies, and are found to have relatively small dispersion in maximum luminosity. For a sample of 6 well-studied type I supernovae in Virgo and 5 in Coma among early-type galaxies where internal absorption is not a problem, Sandage & Tammann (72, 73) found $\Delta m_{cv} = 4.2 \pm 0.3$ mag and $v_v = 40 \pm 160$. If the sample is extended to the supernovae in later-type galaxies, the data are consistent with a substantial velocity field (5), so that the issue is confused.

Tully & Fisher (96) introduced the correlation between luminosity $L$ and 21-cm line-width $\Delta v$ in spiral galaxies, Faber & Jackson (35) the correlation between luminosity and nuclear velocity dispersion $\sigma$ in early galaxies. In the past few years these velocity correlations have been extensively studied in connection with the velocity field problem. Aaronson et al. (4, 5) studied the IR magnitude–$\Delta v$ correlation. For four clusters at redshifts of 4000–6000 km s$^{-1}$ distributed around the sky, they found a uniform Hubble ratio of $95 \pm 4$ km s$^{-1}$. The same technique yielded $65 \pm 4$ for Virgo (5, 51). One interpretation of this result is that the redshift of Virgo underestimates its distance by the factor $\sim 95/65$, which would imply an infall of the Local Group toward Virgo of $520 \pm 75$ km s$^{-1}$. The $L$–$\Delta v$ correlation is quite pronounced with a fairly small scatter of $\sim 0.4$ mag per galaxy. It can be applied to spirals with sky inclination angle greater than $\sim 30$ degrees. The IR $H$ magnitudes are much less affected by dust absorption internal to the galaxy than are $B$ magnitudes, although the Hubble constant anisotropy is seen also when analyzed with the $L_B$–$\Delta v$ correlation (31). Extension of the Aaronson et al. results for more clusters and more galaxies per cluster is in progress, with preliminary results that confirm the isotropy of the Hubble ratio at large distance, now extended to 10,000 km s$^{-1}$ with the inclusion of the Hercules cluster. The preliminary estimate is that $v_v$ is likely to be $\sim 30\%$ lower than the original estimate of Aaronson et al. (private communication).

A similar study was done by Tonry & Davis (92, 93) using the $L$–$\sigma$ correlation for 14 elliptical galaxies inside the Virgo core and 53 ellipticals outside the Virgo core and the triple-value zone. They fit a nonlinear spherical Virgocentric flow model, but most of the comparison ellipticals were outside the LS, so the fit is sensitive mainly to $v_v$. Their result is $v_v = 470 \pm 75$ km s$^{-1}$. A sample of 74 S0 galaxies gave $v_v = 416 \pm 90$ km s$^{-1}$. These results are consistent with the Aaronson et al. study (5).

It has been objected that the Aaronson et al. analysis mixes spirals of all types, while one might look for a different $L$–$\Delta v$ correlation in each morphological class (62, 65). These are refinements for the future, but they do not necessarily vitiate the test.

Another problem is the use of aperture photometry based on diameters derived from blue photographic material (52), which may have systematic errors. Van den Bergh (98) has pointed out that the surface brightnesses of the galaxies are not the same in all the clusters used by Aaronson et al., presumably because of errors in diameters. The interpretation of the Tully-Fisher correlation is somewhat mysterious. Aaronson et al. (1a) interpreted the $L \propto \Delta v^4$ effect as being consistent with (*a*) similarity in the profiles of galaxies with differing luminosity, (*b*) constant mass-to-light ratio, and (*c*) constant central surface brightness. Any two of the above statements implies the third. Statement (*b*) is quite surprising because the spirals all seem to have flat rotation curves and the mass is dominated by the dark halo, whereas the light is not. Burstein (16) has demonstrated that (*c*) is indeed false, more luminous spirals having higher surface brightness. This is a very interesting subject, but it is of course irrelevant to the purpose of finding the velocity field because we seek only an empirical correlation, which the Tully-Fisher relation provides quite well.

The estimates of $v_v$ based on the scaled redshifts of the Virgo cluster depend on the observed redshift. The mean value is well determined (51), but given the observed subclustering and non-Gaussian nature of the redshift distribution, caution is indicated. Yahil (105) suggested that M87, with its enormous X-ray halo, could be at the center of the potential well of Virgo, yet its redshift is larger than the mean by 160 km s$^{-1}$. Adopting this redshift lowers $v_v$ by 160 km s$^{-1}$. However, the asymmetry in the H$\alpha$

emission and radio morphology of the nuclear region of M87 may be caused by a bow-wave induced by a northward motion of M87 in the intracluster medium at a velocity of $\sim 200 \text{ km s}^{-1}$ (32). Given a transverse motion, there is little reason to doubt the possibility of a similar longitudinal motion for M87. Thus the mean redshift still seems to be the best estimate for the Virgo cluster.

## 3.4 *Local Studies*

Galaxies at distances $cz \lesssim 3000$ in the Northern Hemisphere are in or close to the LS, so it is often presumed that the galaxies share an appreciable Virgocentric flow. If so, estimates of the velocity of the Local Group based on the dipole anisotropy for nearby galaxies will tend to underestimate the velocity, while an analysis based on the fit of a large sample to a velocity field model with a few parameters can have good formal statistical accuracy but of course depends on the adequacy of the model. This partly accounts for the checkered history of the subject (25–27, 70). For example, Sandage & Tammann (70), using redshifts and distance estimates of nearby galaxies and groups calibrated by Sc luminosity classes, found that the Hubble ratio shows negligible correlation with position in the sky relative to the LS or with distance toward or away from the LS. De Vaucouleurs (25) repeated his analysis using this new sample and concluded that there is a peculiar velocity field consistent with his earlier result. Peebles (57) found a least-squares fit of the same Sandage-Tammann data to a Virgocentric flow model, keeping only galaxies at distances from the Virgo cluster $> R_1/2$ so as to avoid problems with nonlinear flow. The analysis yielded a local anisotropy that is formally significant within the model, with $v_v = 500 \pm 150 \text{ km s}^{-1}$. It is not clear whether the analysis by Sandage & Tammann of the Hubble ratio should have detected a velocity field this large.

De Vaucouleurs & Peters (30) fit a dipole model to a set of 200 spiral galaxies, using corrected total magnitudes $B_T^0$ and isophotal diameters $D_0$ as distance estimators. Their results do not significantly vary with the mean distance of the sample, broken into subsets of mean redshift 940, 1120, and $2000 \text{ km s}^{-1}$. De Vaucouleurs et al. (31) found a similar result by fitting a dipole model to a sample of 300 spiral galaxies, using a Tully-Fisher correlation with $B_T^0$ magnitudes. In the Virgocentric flow models, the dipole anisotropy at $cz \sim 1000$ is comparable to $v_v$ (to $\sim 20\%$) so we have entered the component of these results directed toward Virgo into Table 1 as estimates of $v_v$, after transforming their results to the Local Group frame used above (107).

Yahil, Sandage, and Tammann (105, 106) used the redshift sample of the revised Shapley-Ames catalog, which is complete to $\sim 13$ mag. They used luminosity alone as a distance indicator, and determined the flow by a redshift-magnitude relation. Yahil found $v_v = 220 \pm 75$ if the redshift of the Virgo cluster is 980 km $s^{-1}$ (105).

The infrared Tully-Fisher method has been applied in two recent local studies. The southern Fornax and Grus groups were used to derive distance moduli relative to Virgo (1). Grus is a diffuse cluster with internal motions not fully separated from the Hubble flow; Fornax is more compact. The relative distance modulus from Fornax to Virgo is $0.03 \pm 0.2$, consistent within the errors of previous studies (5, 101). Although the Grus and Fornax clusters have distances very similar to that of Virgo, their redshifts are considerably higher ($\langle v \rangle = 1340$ km $s^{-1}$ for Fornax corrected to the center of the Local Group). If Fornax is not affected by the Virgocentric flow, the implication is that the Local Group is falling toward Virgo at $v_v = 220 \pm 80$ km $s^{-1}$. If the Virgocentric velocity field varies as $r^{-1}$ to the distance of Fornax, then $v_v = 316 \pm 80$ (1). Similar but slightly higher results were obtained from the Grus cluster.

Aaronson et al. (2) used a sample of 306 field galaxies with $cz < 3000$ km $s^{-1}$ to fit a nonlinear spherical model to the Virgocentric flow plus a three-dimensional random component of velocity for the Local Group. They computed regressions using both redshift and predicted distance as the independent variable. The best infall velocity was $331 \pm 41$ km $s^{-1}$ for the Local Group, with the amplitude of the mean pattern velocity at the position of the Local Group to be $250 \pm 64$ km $s^{-1}$. The separation of the flow pattern into random and systematic components is possible because of the quality of the data set, but the individual components are not as well determined as their sum. The authors found the infall velocity to be moderately sensitive to the power-law dependence of the velocity field, but quite insensitive to the redshift of Virgo or the mean overdensity within our position. The fits are improved if they include differential rotation of the LS, with an amplitude of $180 \pm 58$ km $s^{-1}$ at the radius of the Local Group. This should be compared with $v_s = 297 \pm 25$ from the microwave anisotropy (Equation 9).

## 3.5 *Discussion*

If the local anisotropy of the microwave background is dominated by Virgocentric flow induced by the mass concentration in the LS, the velocity of the Local Group derived from the microwave background ought to point toward the Virgo cluster. The observed velocity is $\sim 45°$ away from the Virgo cluster and 42° away from the local gravity vector (20). Since the LS deviates substantially from spherical symmetry and the flow is unstable against the development of transverse motions, this may not be a fatal disagreement with the gravitational hypothesis. Under this same hypothesis, the entries in Table 1 ought to agree within the errors. The mean of all entries (except 3 and 20) weighted by the stated standard deviations is $v_v = 340$ with $\chi^2 = 58$ for 17 degrees of freedom. Thus if the $v_v$ were all consistent, the standard deviations would have to have been underestimated by a factor of two, which seems unreasonable. If the local estimates are eliminated, we get $v_v = 402$ with $\chi^2 = 23$ for 11 degrees of freedom, which requires that the standard deviations typically are underestimated by 40%, a somewhat more reasonable factor.

The discrepancy of the Rubin velocity with either of the above means is well outside the estimated errors. If the Rubin velocity were valid, the fairly good agreement of $v_v$ from closer objects and the microwave background would have to be an accident. The Hart-Davies result agrees with the microwave background, so we need not invoke an accidental coincidence. We are inclined to give substantially more weight to those studies, such as the Hart-Davies result, that use a second parameter that is distance independent so that the measure is less sensitive to spatial inhomogeneity. Clearly, the debate on this subject will continue.

The estimates at intermediate distance average $v_v = 396$ with $\chi^2 = 21$ for 9 degrees of freedom, which is consistent with the microwave background result. The smallest values of $v_v$ come from the scaling of objects in the Coma and Virgo clusters, and as the environments are so different it is conceivable that the objects are systematically different. Another problem is associated with the structure seen in the redshift distribution of Virgo (33, 44b, 51). This suggests foreground and background objects might have been mixed into the statistics, though the tight distribution seen in the sky would suggest the scatter in distances does not exceed $\sim 10\%$. There is the related problem of defining the observed redshift of the Virgo cluster. As the redshift distribution is broad, and for the spirals does not even show a well-defined peak, the standard estimate (Equation 10) could well be in error. We have indicated in the table those estimates of $v_v$ that are most sensitive to $z_v$.

The local studies are not very sensitive to $z_v$ but do depend on a model for the Virgocentric flow. If the Local Group has an appreciable random motion as well as the general Virgocentric flow, then all entries save the last one in Table 1 may overestimate the pattern velocity. In the linear gravitational pertubation model this effect is not expected, because the gravitational field seems to be dominated by the central concentration of galaxies in the LS (20, 106). A particularly serious problem in the local analyses is the triple-value zone close to Virgo, where the models are doubtful. Inclusion of galaxies in the triple-value zone decreases the infall estimate of Aaronson et al. (2) by $\sim 50$ km s$^{-1}$. If the velocity field of the LS were far from radial even at our Virgocentric radius, then all the local fits would be substantially affected. Further studies clearly are needed to probe the velocity field in as much detail as possible. A distance indicator that may prove useful for this is the IR color-magnitude relation for spiral galaxies (97, 104).

We suspect that the local studies are the least reliable group, so we adopt as the best estimate of $v_v$ the weighted mean of the first 13 estimates in Table 1, excluding entry 3, with the result that

$$v_v = 400 \pm 60 \text{ km s}^{-1}. \tag{11}$$

We have augmented the formal standard deviation in the mean by 40% to make $\chi^2$ reasonable, and then doubled it to take account of the errors common to many of the estimates (particularly the observed redshift of the Virgo cluster). It will be noted that this assumes that all the entries in the table are estimates of the same quantity, and that the stated error of each entry should be adjusted by the same factor. As the latter assumption surely is not true, the standard deviation in Equation 11 likely is an underestimate.

It might be noted that if $v_v \sim 400$ the global value of Hubble's constant is $\sim 40\%$ larger than what is found from the redshift and distance of the Virgo cluster. With standard estimates, this makes the Hubble time $H^{-1}$ less than globular cluster evolution ages (5, 24, 30, 72). If so, the simplest relativistic cosmologies are in trouble, though, as noted by Lemaître (46), they can be saved by the addition of a cosmological constant.



## 4. DYNAMICS OF THE LOCAL SUPERCLUSTER

If $v_v$ is gravitationally induced in a Friedman-Lemaître model with $\Lambda = 0$ the needed mass excess within our radius is $\delta M \sim 3 \times 10^{15}\, \Omega^{0.4}\, h^{-1}\, M_\odot$. This is comparable to typical mass estimates for Abell clusters ($R$ is a factor $\sim 10$ larger, the mean density smaller). Since the mean space density of bright galaxies is $\sim 0.01\ h^3$ Mpc$^{-3}$ (20) and the mean overdensity is $\delta N/N \sim 2$ to 3 (20, 105), the mass per bright galaxy is $\sim 1 \times 10^{13}\ h^{-1}\ M_\odot$. If this mass were in $\rho \sim r^{-2}$ halos at circular velocity 200 km s$^{-1}$, the halo radii would have to be $r \sim 1\ h^{-1}$ Mpc, which goes well beyond the more direct evidence of dark mass around individual galaxies (34). The mass excess per unit volume is $\delta M/V \sim 2 \times 10^{-29}\ \Omega^{0.4}$ g cm$^{-3}$, which is roughly the critical density for a closed model. To estimate the large-scale mean mass density wc need $\delta M/M$. The galaxy concentration is estimated to be $\delta N/N \equiv \delta = 2$ to 3 (20, 105). The mean concentration around Abell clusters is well known; at the radius given by Equations 10 and 11, $\delta_A = 3.0$ (58, 81). As it seems doubtful that the galaxy concentration in the LS is as large as the mean for Abell clusters, which are considerably richer, we adopt $\delta = 2.2 \pm 0.3$. Then if mass and galaxies have the same coarse distribution, the density parameter derived from Figure 1 is $\Omega = 0.35 \pm 0.15$. It should be noted that these numbers depend on the assumption that the local velocity field is induced by the mass concentration, that the mass concentration is approximated by galaxy concentration, and that the Universe behaves like a Friedman-Lemaître model with $\Lambda = 0$.

An important puzzle, and a warning that the spherical models may be too simplistic, is the transverse component of our Virgocentric motion as measured by the microwave anisotropy and other more local studies. The Hart & Davies (43) result is very significant, if true, because it suggests that all of the microwave anisotropy is locally induced. Aaronson et al. (2) also found evidence for transverse velocity, but the amplitude of the transverse velocity is substantially less than that seen in the other works. Because the transverse velocity is close to the Galactic plane, it is difficult to study and the uncertainties are correspondingly larger. On the other hand, the microwave results, which are so frequency independent, almost certainly are not compromised by a Galactic contribution.

A further complication would be evidence for rotation of the Local Supercluster, because the LS is too young to be centripetally supported at our radius, in which case rotational velocities should adiabatically decay as the Universe expands. The recent evidence for rotation (2) was most sensitive to the differential rotation of galaxies closer to Virgo than the Local Group, but another interpretation of these results, as the authors point out, is that nonradial (in Virgocentric frame) peculiar velocities of some of the interior groups can mimic a rotation signal. Such an effect would not be surprising but again warns us of the limitations of the spherical models.



## 5. DIRECTIONS FOR FUTURE RESEARCH

Measurements of the anisotropy of the microwave background have reached a remarkable precision. The anisotropy is so close to dipole that we can see little reason to doubt that it is the result of our peculiar motion in a Universe that is accurately isotropic on the horizon. This measurement alone cannot distinguish between flow on relatively small scales like the LS and currents on scales as large as $\sim 300\, h^{-1}$ Mpc; we must study the galaxy redshift field. The Hubble relation for rich clusters offers an important constraint, but because there is only the Virgo cluster at a convenient distance it is difficult to see how this test can be substantially improved. The local studies depend on a model for the flow, and as the density enhancement even at our radius is substantial it seems unlikely that the spherical models are better than rough indicators of the effect. Studies of more realistic numerical collapse models may prove useful. Because there is only one LS there is the question of reproducibility, though in principle it is possible to check the results by studying the mean flow around a fair sample of clusters. In the intermediate distance studies of the LS, large contributions to $\chi^2$ come from the estimates of the relative distance modulus of the Coma and Virgo clusters. Here future debate is likely to center on the effect of environment on distance indicators. We suspect that a more promising approach is the search for dipole anisotropy in well-distributed galaxy samples at redshifts $\sim$3000–10,000 km s$^{-1}$, as pioneered by Rubin. A particularly promising avenue here is the use of a distance-independent luminosity indicator like the 21-cm line width or infrared color.



## Acknowledgments

This research was supported in part by National Science Foundation grants AST81-18557 and PHY81-18157.

*Literature Cited*

1. Aaronson, M., Dawe, J. A., Dickens, R. J., Mould, J. R., Murray, J. B. 1981. *MNRAS* 195: 1p
1a. Aaronson, M., Huchra, J., Mould, J. R. 1979. *Ap. J.* 229: 1
2. Aaronson, M., Huchra, J., Mould, J. R., Schechter, P. L., Tully, R. B. 1982. *Ap. J.* 258: 64
3. Aaronson, M., Mould, J. 1981. *Publ. Astron. Soc. Pac.* 93: 20
4. Aaronson, M., Mould, J., Huchra, J. 1980. *Ap. J.* 237: 655
5. Aaronson, M., Mould, J., Huchra, J., Sullivan, W., Schommer, R., Bothun, G. 1980. *Ap. J.* 239: 12
6. Aaronson, M., Persson, S. E., Frogel, J. A. 1981. *Ap. J.* 245: 18
7. Abell, G. O. 1974. In *The Formation and Dynamics of Galaxies, IAU Symp. No. 58*, ed. J. R. Shakeshaft, p. 225. Dordrecht: Reidel
8. Abell, G. O. 1975. In *Stars and Stellar Systems*, ed. A. Sandage, M. Sandage, J. Kristian, 9: 601. Univ. Chicago Press
9. Abell, G. O., Eastmond, T. S. 1968. *Astron. J.* 73: 161
10. Abell, G. O., Mihalas, D. M. 1966. *Astron. J.* 71: 635
11. Bautz, L. P., Abell, G. O. 1973. *Ap. J.* 184: 709
11a. Boldt, E. 1981. *Comments Astrophys.* 9: 97
12. Bond, D., Szalay, A., White, S. 1983. *Nature* 301: 584
13. Boughn, S. P., Cheng, E. S., Wilkinson, D. T. 1981. *Ap. J. Lett.* 243: L113
14. Branch, D. 1982. *Ap. J.* 258: 35
15. Branch, D., Bettis, C. 1978. *Astron. J.* 83: 224
16. Burstein, D. 1982. *Ap. J.* 253: 539
17. Byrnes, D. V. 1966. *Publ. Astron. Soc. Pac.* 78: 46
18. Cheng, E. S., Saulson, P. R., Wilkinson, D. T., Corey, B. E. 1979. *Ap. J. Lett.* 232: L139
19. Clutton-Brock, M., Peebles, P. J. E. 1981. *Astron. J.* 86: 1115
20. Davis, M., Huchra, J. 1982. *Ap. J.* 254: 437
21. Davis, M., Peebles, P. J. E. 1983. *Ap. J.* In press
22. Davis, M., Tonry, J., Huchra, J., Latham, D. 1980. *Ap. J. Lett.* 238: L113
23. de Vaucouleurs, G. 1953. *Astron. J.* 58: 30
24. de Vaucouleurs, G. 1958. *Astron. J.* 63: 253
25. de Vaucouleurs, G. 1976. *Ap. J.* 205: 13
26. de Vaucouleurs, G. 1977. *Nature* 266: 126
27. de Vaucouleurs, G., Bollinger, G. 1979. *Ap. J.* 233: 433
28. de Vaucouleurs, G., de Vaucouleurs, A., Corwin, H. 1976. *Second Reference Catalogue of Bright Galaxies*. Austin: Univ. Texas Press
29. de Vaucouleurs, G., Peters, W. L. 1968. *Nature* 220: 868
30. de Vaucouleurs, G., Peters, W. L. 1981. *Ap. J.* 248: 395
31. de Vaucouleurs, G., Peters, W. L., Bottinelli, L., Gougenheim, L., Paturel, G. 1981. *Ap. J.* 248: 408
32. de Young, D. S., Condon, J. J., Butcher, H. 1980. *Ap. J.* 242: 511
33. Eastmond, T. S. 1977. PhD thesis. Univ. Calif., Los Angeles
34. Faber, S. M., Gallagher, J. S. 1979. *Ann. Rev. Astron. Astrophys.* 17: 135

35. Faber, S. M., Jackson, R. E. 1976. *Ap. J.* 204:668
36. Fall, S. M., Jones, B. J. T. 1976. *Nature* 262:457
37. Fixen, D. J. 1982. PhD thesis. Princeton Univ.
38. Deleted in proof
39. Gamow, G. 1946. *Nature* 158:549
40. Gödel, K. 1948. *Rev. Mod. Phys.* 21:447
41. Gorenstein, M. V., Smoot, G. F. 1981. *Ap. J.* 244:361
42. Gunn, J. E. 1978. In *Observational Cosmology*, ed. A. Maeder, L. Martinet, G. Tammann, p. 1. Sauverny: Geneva Obs.
43. Hart, L., Davies, R. D. 1982. *Nature* 297:191
44. Hoffman, G. L., Olson, D. W., Salpeter, E. E. 1980. *Ap. J.* 242:861
44a. Hoffman, G. L., Salpeter, E. E. 1982. *Ap. J.* 266:485
44b. Huchra, J. 1978. *Proc. IAU Symp. 81, The Large-Scale Structure of the Universe*, p. 271
44c. Jackson, R. E. 1982. PhD thesis. Univ. Calif., Santa Cruz
45. Kristian, J., Sachs, R. K. 1966. *Ap. J.* 143:379
46. Lemaître, G. 1933. *Ann. Soc. Sci. Brussels* A53:83
47. Lubin, P. M., Epstein, G., Smoot, G. 1982. *Int. Sch. Phys., Enrico Fermi, 86th Course, Varenna*
48. Lundmark, K. 1924. *MNRAS* 84:747
49. MacCallum, M. A. H. 1979. In *General Relativity*, ed. S. W. Hawking, W. Israel, p. 533. Cambridge Univ. Press
50. Mould, J. 1981. *Publ. Astron. Soc. Pac.* 93:25
51. Mould, J. Aaronson, M., Huchra, J. 1980. *Ap. J.* 238:458
52. Nilsen, P. N. 1973. *Uppsala General Catalogue of Galaxies, Uppsala Astron. Ann. Obs.*, Vol. 6
53. Ogorodnikov, K. F. 1952. *Problems of Cosmogony*, 1:147. Moscow
54. Olson, D. W., Silk, J. 1979. *Ap. J.* 233:395
55. Oort, J. 1939. *Bull. Astron. Neth.* 196:239
56. Partridge, R. B., Wilkinson, D. T. 1967. *Phys. Rev. Lett.* 18:577
57. Peebles, P. J. E. 1976. *Ap. J.* 205:318
58. Peebles, P. J. E. 1980. *The Large-Scale Structure of the Universe*. Princeton Univ. Press
59. Peebles, P. J. E. 1981. *Ap. J. Lett.* 243:L119
60. Peebles, P. J. E., Wilkinson, D. T. 1968. *Phys. Rev.* 174:2168
61. Raychaudhuri, A. 1955. *Phys. Rev.* 98:1123
62. Roberts, M. S. 1978. *Astron. J.* 83:1026
63. Rubin, V. C. 1952. MSc thesis. Cornell Univ.
64. Rubin, V. C. 1952. *Astron J.* 56:47
64a. Rubin, V. C. 1976. In *IAU Colloq. No. 37, Décalages vers Rouge et Expansion de l'Univers*. Paris: Cent. Natl. Rech. Sci.
65. Rubin, V. C., Burstein, D., Thonnard, N. 1980. *Ap. J. Lett.* 242:L149
66. Rubin, V. C., Ford, W. K., Rubin, J. S. 1973. *Ap. J. Lett.* 183:L111
67. Rubin, V. C., Thonnard, N., Ford, W. K., Roberts, M. S. 1976. *Astron. J.* 81:719
68. Sandage, A. 1972. *Ap. J.* 178:1
69. Sandage, A. 1973. *Ap. J.* 183:731
69a. Sandage, A., Kristian, J., Westphal, J. A. 1976. *Ap. J.* 205:688
70. Sandage, A., Tammann, G. A. 1975. *Ap. J.* 196:313
71. Sandage, A., Tammann, G. A. 1976. *Ap. J.* 210:7
72. Sandage, A., Tammann, G. A. 1982. In *Astrophysical Cosmology, Scripta Varia*, 48:23
73. Sandage, A., Tammann, G. A. 1982. *Ap. J.* 256:339
74. Sandage, A., Tammann, G. A., Hardy, E. 1972. *Ap. J.* 172:253
75. Sandage, A., Visvanathan, N. 1978. *Ap. J.* 223:707
76. Sandage, A., Visvanathan, N. 1978. *Ap. J.* 225:742
77. Schechter, P. L. 1977. *Astron. J.* 82:569
78. Schechter, P. L. 1980. *Astron. J.* 85:801
79. Schücking, E. 1957. *Naturwissenschaften* 44:507
80. Sciama, D. W. 1967. *Phys. Rev. Lett.* 18:1065
81. Seldner, M., Peebles, P. J. E. 1977. *Ap. J.* 215:703
82. Shapley, H. 1923. *MNRAS* 94:791
83. Silk, J. 1974. *Ap. J.* 193:525
84. Silk, J. 1977. *Astron. Astrophys.* 59:53
85. Silk, J., Szalay, A. 1983. *Ap. J. Lett.* 264:L31
86. Silk, J., Wilson, M. L. 1981. *Ap. J. Lett.* 244:L37
87. Smoot, G., Lubin, P. M. 1979. *Ap. J. Lett.* 234:L83
88. Deleted in proof
89. Stewart, J. M., Sciama, D. W. 1967. *Nature* 216:748
90. Tammann, G. A., Sandage, A., Yahil, A. 1979. *Ap. J.* 234:775
91. Tifft, W. G., Gregory, S. A. 1976. *Ap. J.* 205:696
92. Tonry, J. L., Davis, M. 1981. *Ap. J.* 246:666
93. Tonry, J. L., Davis, M. 1981. *Ap. J.* 246:680
94. Truman, A. H. 1916. *Pop. Astron.* 24:11
95. Tully, R. B. 1982. *Ap. J.* 257:389
96. Tully, R. B., Fisher, J. R. 1977. *Astron. Astrophys.* 54:661

97. Tully, R. B., Mould, J., Aaronson, M. 1982. *Ap. J.* 257:527
98. van den Bergh, S. 1981. *Ap. J. Lett.* 248:L9
99. Visvanathan, N. 1979. *Ap. J.* 228:81
100. Visvanathan, N., Griersmith, D. 1979. *Ap. J.* 230:1
101. Visvanathan, N., Sandage, A. 1977. *Ap. J.* 216:214
102. Weedman, D. W. 1976. *Ap. J.* 203:6
103. White, S. D. M., Silk, J. 1979. *Ap. J.* 231:1
104. Wyse, R. 1982. *MNRAS* 199:1
105. Yahil, A. 1981. *10th Texas Symp. Relativ. Astrophys.*, ed. R. Ramaty, F. C. Jones. *Ann. NY Acad. Sci.* 375:169
106. Yahil, A., Sandage, A., Tammann, G. A. 1980. *Ap. J.* 242:448
107. Yahil, A., Tammann, G. A., Sandage, A. 1977. *Ap. J.* 217:903
108. Zel'dovich, Ya. B. 1970. *Astron. Astrophys.* 5:84